

## **Eyeblink conditioning performance and brain-wide *C-fos* expression in male and female mice**

Maria Roa Oyaga<sup>1#</sup>, Ines Serra<sup>1#</sup>, Devika Kurup<sup>1</sup>, Sebastiaan K.E. Koekkoek<sup>1</sup>, Aleksandra Badura<sup>1,2</sup>

<sup>1</sup> Department of Neuroscience, Erasmus MC, 3000 Rotterdam, the Netherlands

<sup>2</sup> Netherlands Institute for Neuroscience, Royal Dutch Academy for Arts and Sciences, Amsterdam, the Netherlands

# These authors contributed equally to this work

1 **Abstract**

2           The functional and molecular sources of behavioral variability in mice are not fully understood. As a  
3 consequence, the predominant use of male mice has become a standard in animal research, under the assumption  
4 that males are less variable than females. Similarly, to homogenize genetic background, neuroscience studies have  
5 almost exclusively used the C57BL/6 (B6) strain. Here, we examined individual differences in performance in the  
6 context of associative learning. We performed delayed eyeblink conditioning while recording locomotor activity in  
7 mice from both sexes in two strains (B6 and B6CBAF1). Further, we used a C-FOS immunostaining approach to  
8 explore brain areas involved in eyeblink conditioning across subjects and correlate them with behavioral  
9 performance. We found that B6 male and female mice show comparable variability in this task and that females  
10 reach higher learning scores. We found a strong positive correlation across sexes between learning scores and  
11 voluntary locomotion. C-FOS immunostainings revealed positive correlations between C-FOS positive cell density  
12 and learning in the cerebellar cortex, as well as multiple previously unreported extra-cerebellar areas. We found  
13 consistent and comparable correlations in eyeblink performance and *C-fos* expression in B6 and B6CBAF1 females  
14 and males. Taken together, we show that differences in motor behavior and activity across brain areas correlate with  
15 learning scores during eyeblink conditioning across strains and sexes.

16

## 17 **Introduction**

18 For several decades, female mice have been considerably under-investigated in neuroscience due to the  
19 presumption that hormonal fluctuations caused by the estrous cycle might introduce non-comparable variability  
20 across sexes (Meziane et al., 2007). However, meta-analyses of rat and mice studies show that females and males  
21 exhibit comparable variability across behavioral, morphological and physiological traits, and that for most traits,  
22 female estrous cycle does not need to be considered (Simpson and Kelly, 2012; Becker et al., 2016).  
23 Notwithstanding, female and male mice show sex-specific strategies in locomotion adaptation, reward learning, and  
24 spatial orientation and learning (Konhilas et al., 2004; Bettis and Jacobs, 2009; Hendershott et al., 2016; Grissom  
25 et al., 2018; Prawira, 2019).

26 The development of inbred mouse strains was also intended to decrease the variability between animals and  
27 increase the power of studies (Festing, 1999). However, the current golden standard to keep mice exclusively on  
28 the C57BL/6 (B6) strain, limits the generalization of findings (Rivera and Tessarollo, 2008; Sittig et al., 2016).  
29 When it comes to inter-strain variability, behavioral differences have been reported, yet, it has not been  
30 systematically investigated across commonly used paradigms (Faure et al., 2017; Arnold and Newland, 2018).

31 Although some components of murine behavioral variability have been extensively studied, a number of  
32 variables that could alter learning are largely unexplored (Pfaff, 2001; Bucán and Abel, 2002; Tye et al., 2011;  
33 Leung and Jia, 2016). Hence, gaining a deeper understanding of the sources of behavioral variability could give us  
34 indications on how to interpret data and ensure better reproducibility across laboratories.

35 In order to study how sex and strain influence mouse behavior and brain activity, a reliable and controlled  
36 paradigm is needed. We investigated this in the context of delay eyeblink conditioning. Eyeblink conditioning is a  
37 cerebellar-dependent associative learning paradigm, in which an initially neutral, conditioned stimulus (CS, a  
38 flashing light), becomes predictive of an unconditioned stimulus (US, an air-puff to the cornea), which elicits a  
39 blink. The paradigm consists of pairing the CS with the US and, over time, an association is formed where blinking  
40 is triggered by the CS alone. The newly learned association is called conditioned response (CR) (Gormezano et al.,  
41 1962).

42           There is limited knowledge on sex-related performance differences in eyeblink conditioning. In human  
43 delay eyeblink studies, girls show more CRs in the first five days of learning compared to boys, and women show  
44 a continuous increase in CRs compared to men (Löwgren et al., 2017). In rats, stress seems to enhance delay  
45 eyeblink conditioning in males but hinders learning in females (Wood and Shors, 1998). However, in rabbits, males  
46 and females show similar conditioning profiles but females seem to adapt faster to stress (Schreurs et al., 2018).  
47 Finally, in mice, females show increased CRs compared to males in the first five days of learning trace conditioning  
48 (Rapp et al., 2021), a different form of eyeblink conditioning where a CS and US are separated in time. Comparison  
49 of performance differences in eyeblink conditioning in different strains is currently lacking.

50           At the circuit level, studies have shown that the association between the stimuli during delay eyeblink  
51 conditioning most likely relies on the cerebellum. Here, the CS signals coming from the pons and the CS information  
52 from the inferior olive via climbing fibers are precisely timed and processed (Heiney et al., 2014a; ten Brinke et al.,  
53 2015). Several cerebellar areas modulating eyeblink conditioning have been identified in mice; lobule VI in the  
54 vermal region and crus 1 and simplex in the hemispheric region (Heiney, Kim, et al., 2014; Gao et al., 2016).  
55 Inactivation of lobule VI and crus 1 during development causes deficits in learning, indicating a crucial role in  
56 eyeblink conditioning (Badura et al., 2018). The CR signal leaves the cerebellum via the interposed nucleus, which  
57 ultimately connects to the muscles controlling the eyeblink reflex (Gao et al., 2016; ten Brinke et al., 2017). Beyond  
58 the pontocerebellar and olivocerebellar systems, little is known about the potential involvement of other brain areas  
59 in eyeblink conditioning (Boele et al., 2010; Ruigrok, 2011; D'Angelo et al., 2016; Kratochwil et al., 2017). The  
60 amygdala has been proposed to have a role in associative learning, given its implication in fear conditioning and  
61 arousal (Lee and Kim, 2004). Specifically, lesions in the amygdala during the first days of training highly impair  
62 learning, while lesions in later stages do not appear to affect learning (Lee and Kim, 2004).

63           Our understanding of behavioral variability and engagement of different brain regions is finally limited by  
64 the practise of outliers removal - animals that deviate from the group mean and do not reach proficient learning  
65 scores are commonly dropped from further analysis (Osborne and Overbay, 2004; Rousselet and Pernet, 2012;  
66 Fonnesu and Kuczewski, 2019). Possible mechanisms underlying performance differences could be arousal levels  
67 and locomotor activity, which both influence cortical function (McGinley et al., 2015; Vinck et al., 2015;

68 Williamson et al., 2015), or stress levels which can affect neuronal firing in the deep cerebellar nuclei (DCN) and  
69 hippocampus (Joëls, 2009; Schneider et al., 2013). In the cerebellum, although locomotion modulates activity in  
70 the cortex, the relevance of this modulation is still not fully understood (Ozden et al., 2012; Hoogland et al., 2015;  
71 Powell et al., 2015). During eyeblink conditioning, imposed locomotor activity enhances learning by increased  
72 activation of the mossy fiber pathway to the cerebellar cortex (Albergaria et al., 2018).

73 Here, we investigated the effect of sex in behavioral variability by employing eyeblink conditioning to  
74 quantify performance differences in B6 mice and B6CBAF1 mice. Furthermore, we explored the engagement of  
75 brain regions that may have a modulatory role in eyeblink conditioning by utilizing *C-fos* expression as a proxy for  
76 neural activity during learning in both of those strains. We found that male and female mice of both B6 and  
77 B6CBAF1 strains showed comparable variability in the delay eyeblink conditioning. However, females reached  
78 higher learning scores. Further, we found a strong positive correlation across sexes between learning scores and  
79 voluntary locomotion in the B6 mice. C-FOS immunostaining revealed positive correlations between C-FOS  
80 positive cell density and learning in the cerebellar cortex, as well as multiple previously unreported extra-cerebellar  
81 areas.

82  
83

## 84 **Results**

### 85 *B6 female and male mice show comparable variability in eyeblink conditioning and females reach higher learning* 86 *scores*

87 To study differences in learning profiles between sexes, we performed delayed eyeblink conditioning  
88 experiments with B6 females ( $n = 14$ ) and males ( $n = 14$ ). First, we habituated the animals to the set-up for increasing  
89 periods of time over five days to decrease anxiety levels and optimize training. Next, we subjected mice to a 5-day  
90 training paradigm in order to capture behavioral variability in the first stages of learning. This training length was  
91 selected considering that animals show the most variability within the first days of acquisition, start showing reliable  
92 CRs in day four/five and eventually plateau during the last 5 days of training (Heiney et al., 2014b; Giovannucci et  
93 al., 2017).

94 The blue LED light (CS) was triggered 250 ms prior to the puff to the cornea (US) in paired trials and the  
95 two stimuli co-terminated (**Fig. 1A**). Sessions consisted of 20 blocks of 12 trials each (1 US only, 11 paired and 1  
96 CS only). Mice learned the association between the stimuli progressively and developed a gradually increasing  
97 conditioned response (CR) (**Fig 1A, 1B**). Males and females had comparable learning profiles, and the variances  
98 during training sessions were not significantly different between sexes (F-test for two sample variances in CR  
99 amplitude of paired trials,  $F = 3.66$ ,  $p = 0.11$ ). In CS only trials, females showed a slight increase in CR percentage  
100 on session four, that culminated with a 60% CR responses in session five opposed to 40% in males (two-way  
101 ANOVA repeated measures for sex and sessions: sex effect:  $F(1,26) = 1.461$ ,  $p = 0.24$ , interaction sex and session:  
102  $F(4,104) = 4.01$ ,  $p = 0.02$ , Cohen's  $d$  session five: 0.88) (**Fig. 1C**). The CR amplitude (measured as the response  
103 normalized to UR max amplitude = 1) during CS trials was significantly higher in females compared to males (two-  
104 way ANOVA repeated measures for sex and sessions: sex effect:  $F(1,26) = 6.109$ ,  $p = 0.02$ , interaction sex and  
105 session:  $F(4,104) = 5.12$ ,  $p = 0.0008$ , Cohen's  $d$  session five: 0.93) (**Fig. 1D**). On the last session of training, females  
106 reached an average amplitude of 0.55 while males reached an average of 0.33 (**Fig. 1E**). Overall, these results show

107 that male and female mice show comparable variance in eyeblink conditioning, but females reach higher learning  
108 scores in a 5-day training paradigm.

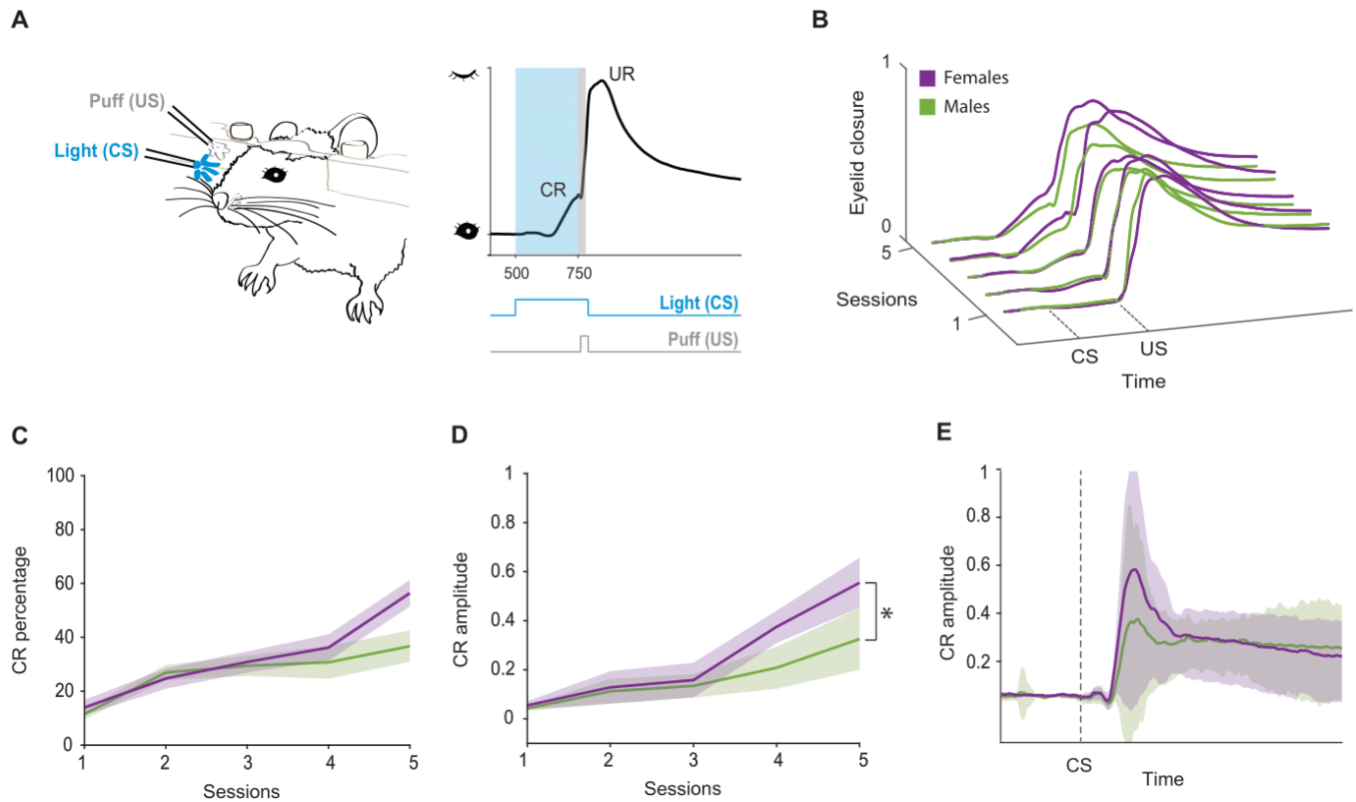


**Figure 1:** B6 female and male mice show comparable variability in eyeblink conditioning and females reach higher learning scores. A) Experimental setup. Mouse with implanted headplate is head-fixed on top of a freely rotating wheel. A blue light (conditioned stimulus, CS) is presented 250 ms before a puff (unconditioned stimulus, US) to the same eye. In a trained mouse, the CS produces an anticipatory eyelid closure (conditioned response, CR) followed by a blink reflex triggered by the US (unconditioned response, UR). B) Paired trails average traces in females and males over training sessions. The CR progressively develops due to the CS-US pairing. C) CR percentage in CS only trials over training sessions. Purple: females, green: males. Shaded area: sem. D) CR amplitude in CS only trials over training sessions (two-way ANOVA for sex and sessions: sex effect:  $F(1,26) = 6.109$ ,  $p = 0.02$ ) Shaded area: sem. E) Average response in CS only trials in the last session of training. Purple: females ( $n=14$ ), green: males ( $n=14$ ). Shaded area: std.

109 *Learning scores correlate with spontaneous locomotor activity*

110

111

112

113

114

We next asked whether mice show behavioral differences in voluntary locomotor activity during training, as it has been shown that imposed locomotion affects eyeblink performance (Albergaria et al., 2018). We investigated whether higher learning scores would correlate with higher spontaneous locomotor activity. For this purpose, we added infrared cameras to the eyeblink setups to record body movements during eyeblink sessions. The

115 cameras were placed at the right back corner of the box, allowing a wide recording angle to capture whole body  
116 movements (**Fig. 2A**). We recorded videos of full training sessions for each mouse, which were later analyzed  
117 offline. The head bar height (**Fig. 1A**) was adjusted accordingly to ensure that every mouse could move comfortably  
118 on the wheel.

119 To track different body parts and get a meaningful movement output, we used DeepLabCut (DLC), a  
120 software for automated animal pose tracking (Mathis et al., 2018) (Materials and Methods; *Movement analysis*).  
121 This approach allows movement tracking without utilizing physical markers on the body that can hinder natural  
122 movement. We tracked 5 body parts: tail base, hip, knee, right back paw and nose (**Fig. 2A**). Animals were head-  
123 fixed on top of the wheel, hence, Y position was similar between both sexes (**Fig 2. B, C**). We observed more  
124 fluctuation in the hip and tail along the X axis in males, which might indicate a tendency to rotate their body axis  
125 from side to side (**Fig 2. B,C**). We selected speed of the right back paw as a proxy for general locomotion behavior  
126 on further analysis.

127 Animals increased their speed on the wheel during training, and both females and males had comparable  
128 variances (F-test for two sample variances in speed:  $F = 0.58, p = 0.305$ ). We found that females moved significantly  
129 faster than males during learning, reaching an average speed of 31 cm/s compared to males that reached 24 cm/s  
130 (two-way ANOVA repeated measures for sex and sessions: sex effect:  $F(1,26) = 12.17, p = 0.0017$ , Cohen's d  
131 session five: 1.07) (**Fig. 2D, E**). Because we observed a similar trend between CR amplitude and running speed  
132 across sexes, we performed a linear regression between speed of the right back paw and CR amplitude in the last  
133 session. This showed a clear correlation between the variables ( $R^2 = 0.75, p = 0.002$ ) (**Fig.2 F**). These results reveal  
134 that mice that spontaneously move faster on the wheel, reach higher learning scores in eyeblink conditioning.



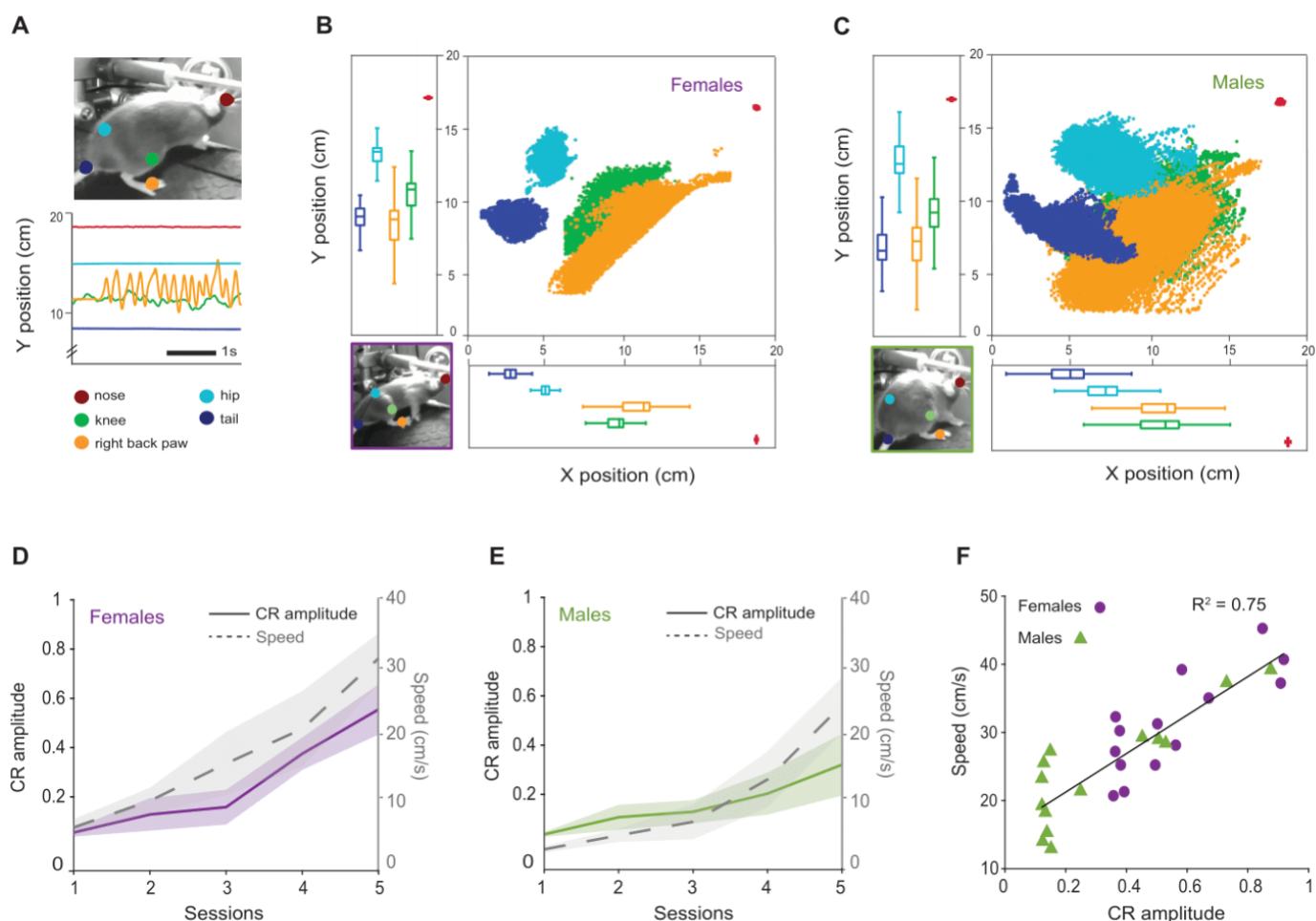


**Figure 2:** Learning scores correlate with spontaneous locomotor activity. A) Top: Example view of tracking with DeepLabCut. Bottom: Example tracking traces (Y position change). B) Scatter plot and boxplots of each body part (females,  $n = 14$ ). C) Scatter plot and boxplots of each body part (males,  $n = 14$ ). D and E) CR amplitude and speed of the right back paw over training sessions. Purple: females ( $n = 14$ ), green: males ( $n = 14$ ). Shaded area: sem. Speed: two-way ANOVA for sex and sessions: sex effect:  $F(1,26) = 12.17$ ,  $p = 0.0017$ . F) Positive correlation between CR amplitude and speed of the right back paw on the last session of training (linear regression:  $R^2 = 0.75$ ,  $p = 0.002$ ).

135

136 *Learning scores correlate with C-fos expression*

137

138

To explore if differences in eyeblink performance correlate with differences in brain activity, we performed

139 C-FOS immunostainings following the last training session. *C-fos* is an immediate early expressed gene, a family

140 of transcription factors that is expressed shortly after a neuron has depolarized. Because of its precise time window

141 of expression, it is widely used as an activity marker (Chung, 2015). Evidence suggests that C-FOS protein greatly

142 increases after exposure to novel objects, surroundings or stimuli, while continuous, long-term exposure to

143 persistent stimuli returns *C-fos* expression to basal levels (Joo et al., 2015; Gallo et al., 2018; Bernstein et al., 2019).  
144 Besides our aim to capture the variability in the first stages of learning, the *C-fos* expression due to novelty was  
145 another reason to choose a 5-day training paradigm instead of the standard 10-day acquisition training.

146 We imaged sections of whole brains with a fluorescent microscope and developed an image analysis  
147 workflow to quantify C-FOS positive neurons and identify their location within the hierarchical structure of the  
148 Allen Brain Atlas (cerebrum, brainstem and cerebellum). (**Supp. Fig. 1**).

149 To identify regions potentially involved in associative learning, we selected mice that showed a CR  
150 amplitude of 0.4 or higher in CS only trials (n = 14; 5 B6 males, 9 B6 females). These mice are further referred as  
151 “learners”. We performed Kendall's correlation (non-parametric rank order regression) between density of C-FOS  
152 positive cells and CR amplitude on the last session. In the cerebellum, C-FOS labeling was localized in the granule  
153 cell layer, which we confirmed with colocalization with GABA $\alpha$ 6, a granule cell specific marker (**Fig 3A, Supp**  
154 **Fig. 2, Supp Fig. 3 A, B**). In the cerebellar hemispheric regions, crus 1 and simplex had a significant correlation  
155 between C-FOS cell density and CR amplitude (crus 1: tau = 0.42,  $p = 0.042$ , simplex: tau = 0.52,  $p = 0.009$ ). In the  
156 cerebellar vermis, lobule VI also had a significant correlation and the highest Tau (lobule VI: tau = 0.8,  $p = 0.009$ )  
157 (**Fig. 3B**). In the brain stem, we found a significant correlation in the red nucleus, the facial nucleus, the inferior  
158 olive and the pontine nuclei (Red nucleus: tau = 0.43,  $p = 0.041$ , Facial nucleus: tau = 0.57,  $p = 0.006$ , inferior  
159 olive: tau = 0.76,  $p = 0.0008$ , pontine nuclei: tau = 0.48,  $p = 0.021$ ) (**Fig. 3E, Supp Fig. 2**). We found a positive  
160 correlation in the visual, motor and somatosensory cortices, and the amygdala (visual cortex: tau = 0.51,  $p = 0.013$ ,  
161 motor cortex: tau = 0.69,  $p = 0.0003$ , somatosensory cortex: 0.54,  $p = 0.007$ , amygdala: tau = 0.63,  $p = 0.001$ ) (**Fig.**  
162 **3H, Supp Fig. 2**). Finally, to understand whether there was a certain layer specificity in these cortices, we performed  
163 two double immunostainings with C-FOS; CUX1, a marker for upper cortical layers (II-IV) and CTIP2, for lower  
164 cortical layers (V-VI). Although we detected C-FOS positive cells in all layers of the cortex, we observed a higher  
165 colocalization of CUX1 and C-FOS compared to CTIP2 and C-FOS (**Supp Fig. 3 C-F**).

166 Together, these results confirm the previously reported areas associated with eyeblink conditioning within  
 167 the olivo-cerebellar and ponto-cerebellar systems (Ruigrok, 2011; D'Angelo et al., 2016) and suggest that other  
 168 areas might be involved in this learning task.

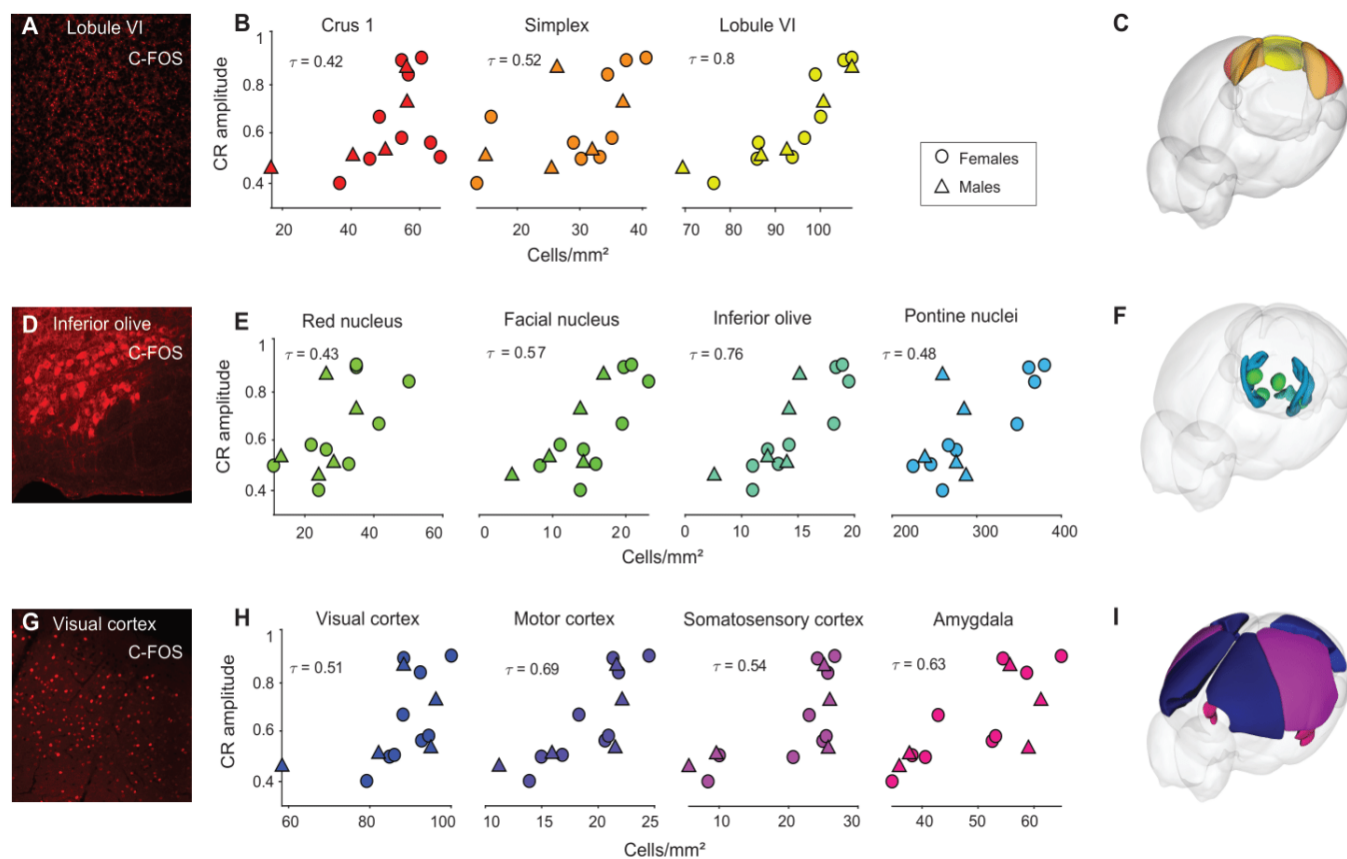


**Figure 3:** Learning scores correlate with *C-fos* expression. **A)** C-FOS positive granule cells in lobule VI in the cerebellum. **B)** Cerebellar areas with significant positive correlation between C-FOS positive cell density and CR amplitude (crus 1: tau = 0.42,  $p = 0.042$ , simplex: tau = 0.52,  $p = 0.009$ , lobule VI: tau = 0.8,  $p = 0.009$ ). **C)** 3D model with significant areas highlighted. **D)** C-FOS positive cells in the inferior olive. **E)** Brainstem areas with significant positive correlation between C-FOS positive cell density and CR amplitude (red nucleus: tau = 0.43,  $p = 0.041$ , facial nucleus: tau = 0.57,  $p = 0.006$ , inferior olive: tau = 0.76,  $p = 0.0008$ , pontine nuclei: tau = 0.48,  $p = 0.021$ ). **F)** 3D model with significant areas highlighted. **G)** C-FOS positive cells in the visual cortex. **H)** Cortical areas with significant positive correlation between C-FOS positive cell density and CR amplitude (visual cortex: tau = 0.51,  $p = 0.013$ , motor cortex: tau = 0.69,  $p = 0.0003$ , somatosensory cortex: 0.54,  $p = 0.007$ , amygdala: tau = 0.63,  $p = 0.001$ ). **I)** 3D model with significant areas highlighted.

169 *Pseudoconditioned mice show lower C-fos expression*

170

171 To ensure an appropriate control for the quantification of C-FOS positive cells, we included  
 172 pseudoconditioned mice (n = 2 B6 males, 2 B6 females) in our experimental design. These mice went through the

173 same experimental steps as the conditioned mice, with the only exception that they were not trained with paired CS-  
174 US trials. Instead, we exposed them to a protocol with CS and US only trials, keeping the same structure and  
175 duration as the conditioned protocol. Pseudoconditioned mice did not acquire an association given that there was  
176 no substrate for learning (absence of CS-US pairing) and exhibited a slight increase in locomotion speed over  
177 training sessions (**Fig. 4A**). We used the same analysis method to quantify the density of C-FOS positive cells in  
178 pseudoconditioned mice. Overall, we observed lower *C-fos* expression in pseudoconditioned mice compared to  
179 learners (**Fig. 4B**). We compared the C-FOS density between pseudoconditioned mice and learner mice in the areas  
180 where we had found a positive significant correlation between CR amplitude and C-FOS density (**Fig. 3**). Learners  
181 had a higher C-FOS density median compared to pseudoconditioned mice (**Fig. 4C**). We found a significant  
182 difference between the groups in each one of these areas (Two-tailed Mann-Whitney U test between  
183 pseudoconditioned and learner mice; crus 1:  $p = 0.00008$ , simplex:  $p = 0.00008$ , lobule VI:  $p = 0.00008$ , red nucleus:  
184  $p = 0.00008$ , facial nucleus  $p = 0.01$ , inferior olive:  $p = 0.00008$ , pontine nucleus:  $p = 0.00008$ , visual cortex:  $p =$   
185  $0.00008$ , motor cortex:  $p = 0.0002$ , somatosensory cortex:  $p = 0.03$ , amygdala:  $p = 0.001$ ) (**Fig. 4D**). This confirms  
186 that the observed increased *C-fos* expression in learner mice is due to the CS-US pairing.

187

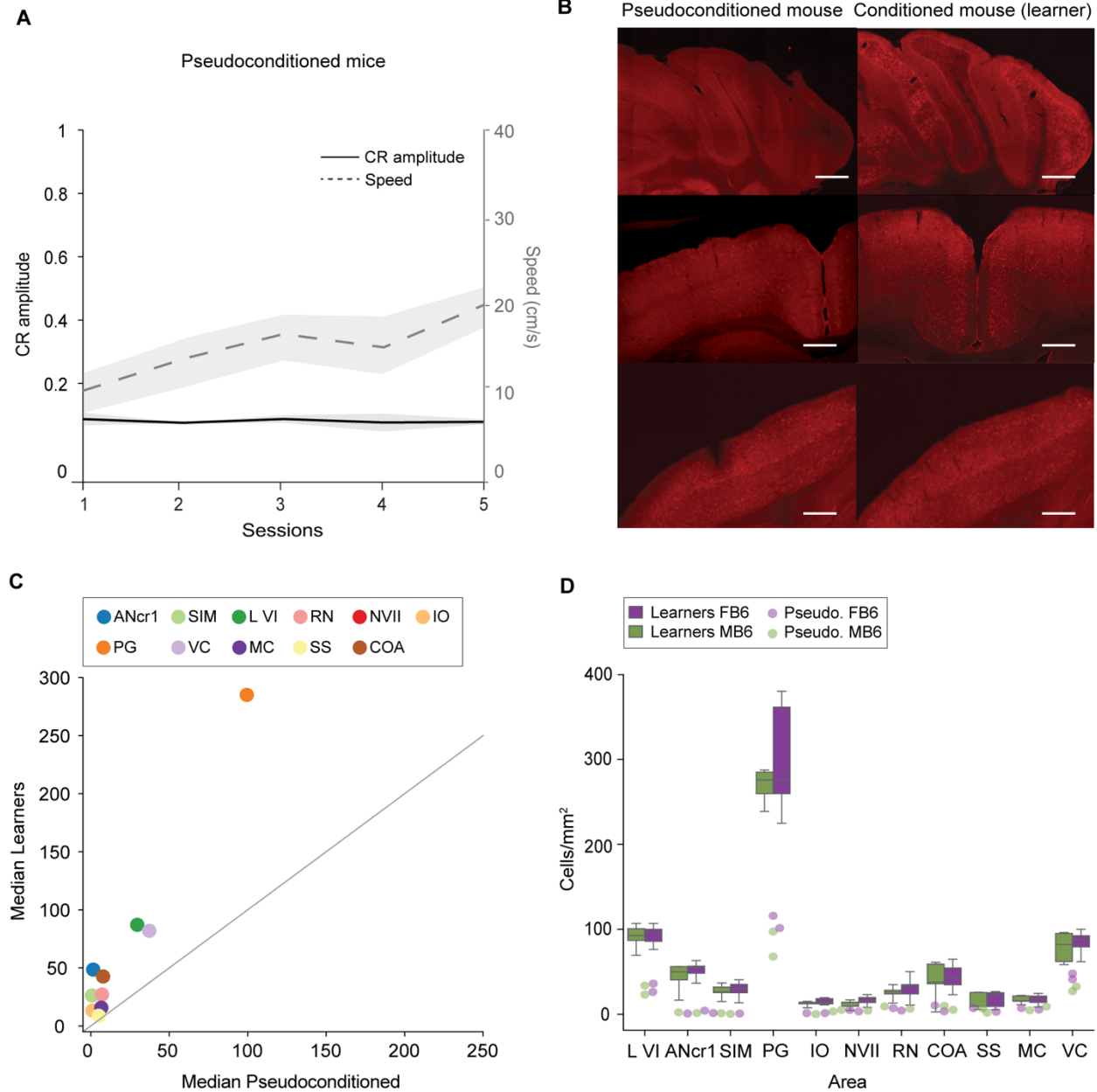


**Figure 4:** Pseudoconditioned mice show lower *C-fos* expression compared to learners. **A)** Change in CR amplitude and Speed of the right back paw over training sessions. CR amplitude left Y axis in black, Speed, in the right Y axis in grey. **B)** Immunofluorescent images, C-FOS positive cells. Top to bottom: cerebellar cortex, motor cortex, somatosensory cortex. Scale bar: 100  $\mu$ m. **C)** Median pseudoconditioned mice against median learners, unity line in grey. **D)** Boxplots depict C-FOS density in learners (n = 9 females, 5 males), dots are pseudoconditioned mice (n = 2 females, 2 males). Green males, purple females. Brain area acronyms from the Allen Brain Atlas: SIM: simplex, ANcr1: crus 1, L VI: lobule VI, RN: red nucleus, NVII: facial nucleus, IO: inferior olive, PG: pontine nucleus, VC: visual cortex, MC: motor cortex, SS: somatosensory cortex, COA: amygdala.

190 *Correlation between learning scores and C-fos expression is consistent in B6CBAF1 strain*  
191

192         Given the evidence of the possible unwanted effects of highly inbred mouse strains like B6 in replicability  
193 and reproducibility (Åhlgren and Voikar, 2019), we wanted to investigate inter-strain variability in associative  
194 learning. We asked whether the results obtained in B6 mice would be consistent in a different mouse strain. For this  
195 purpose, we performed eyeblink conditioning together with C-FOS immunostainings in B6CBAF1 mice, which are  
196 the F1 hybrids of B6 and CBA strains. Hybrid mice are used due to their hybrid vigor, the robustness and health  
197 gained from a high degree of heterozygosity (Wolfer et al., 2002). B6CBAF1 mice have significantly less retinal  
198 degeneration and hearing loss compared to B6 mice, which makes them an appropriate candidate for visual and  
199 auditory experiments (Erway et al., 1996; Milon et al., 2018; Ohlemiller, 2019).

200         B6CBAF1 mice learned the association between the stimuli and gradually formed CRs. We observed a  
201 trend indicating similar sex differences between B6CBAF1 mice and B6. Females reached 53% CR percentage  
202 compared to 35% in males (two-way ANOVA repeated measures for sex and sessions: sex effect:  $F(1,14) = 2.55$ ,  
203  $p = 0.237$ , interaction sex and session:  $F(4,104) = 3.01$ ,  $p = 0.021$ , Cohen's d session five: 0.86) (**Fig 5. A**). When  
204 it comes to the amplitude of these responses, BFCBAF1 females showed a trend towards slightly higher CR  
205 amplitude over training sessions compared to males (two-way ANOVA repeated measures for sex and sessions: sex  
206 effect:  $F(1,14) = 2.55$ ,  $p = 0.132$ , Cohen's d session five: 0.84 ) (**Fig 5. B**).

207         We followed the same analysis pipeline to quantify *C-fos* expression in brain slices of B6CBAF1 mice after  
208 eyeblink conditioning. Next, we selected mice that showed a CR amplitude of 0.4 or higher in CS only trials (n=11;  
209 3 males, 8 females) and performed Kendall's correlation between density of C-FOS positive cells and CR amplitude  
210 on the last training session. The granule cell layer also contained C-FOS labelling, and crus 1, the simplex and  
211 lobule VI were found to have a significant positive correlation (crus 1: tau = 0.82,  $p = 0.0001$ , simplex: tau = 0.7,  $p$   
212 = 0.005, lobule VI: tau = 0.75,  $p = 0.0007$ ) (**Fig 5. C, D, Supp Fig. 5**). In the hindbrain, the correlation between C-  
213 FOS cells and learning was also significant in the inferior olive and the pontine nuclei (inferior olive: tau = 0.85,  $p$   
214 = 0.0004, pontine nuclei: tau = 0.78,  $p = 0.0003$ ) (**Fig 5. E, F, Supp Fig. 5**). Additionally, the visual, motor and  
215 somatosensory cortices showed significant positive correlations (visual cortex: tau = 0.64,  $p = 0.0057$ , motor cortex:



216 tau = 0.75  $p = 0.0008$ , somatosensory cortex: tau = 0.6,  $p = 0.009$ ) (Fig 5. G, H, Supp Fig. 5). These results show  
 217 that most of the areas where we saw a correlation between learning and C-FOS density in B6 mice are also found  
 218 in B6CBAF1 mice, which strengthens the idea that these areas are active during eyeblink conditioning.

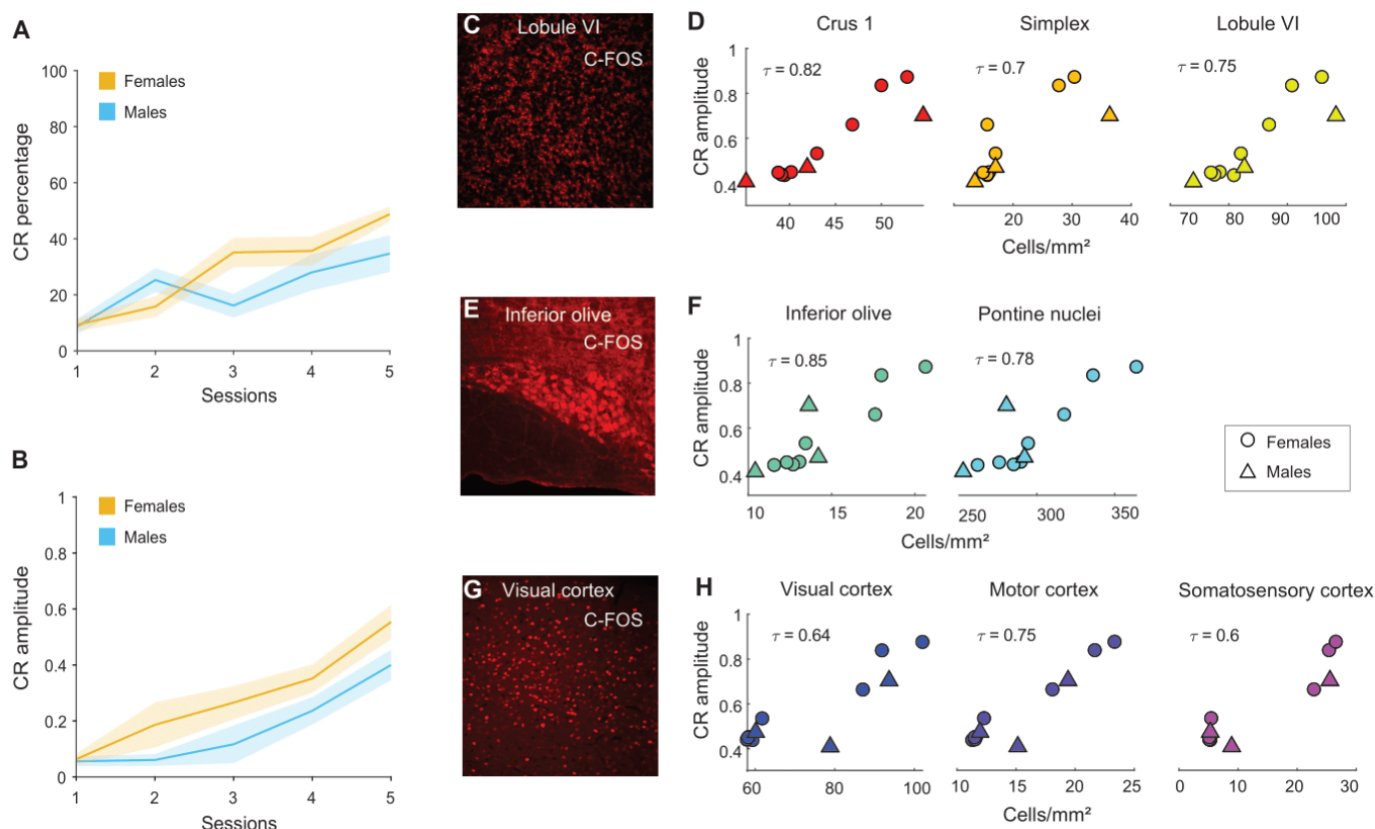
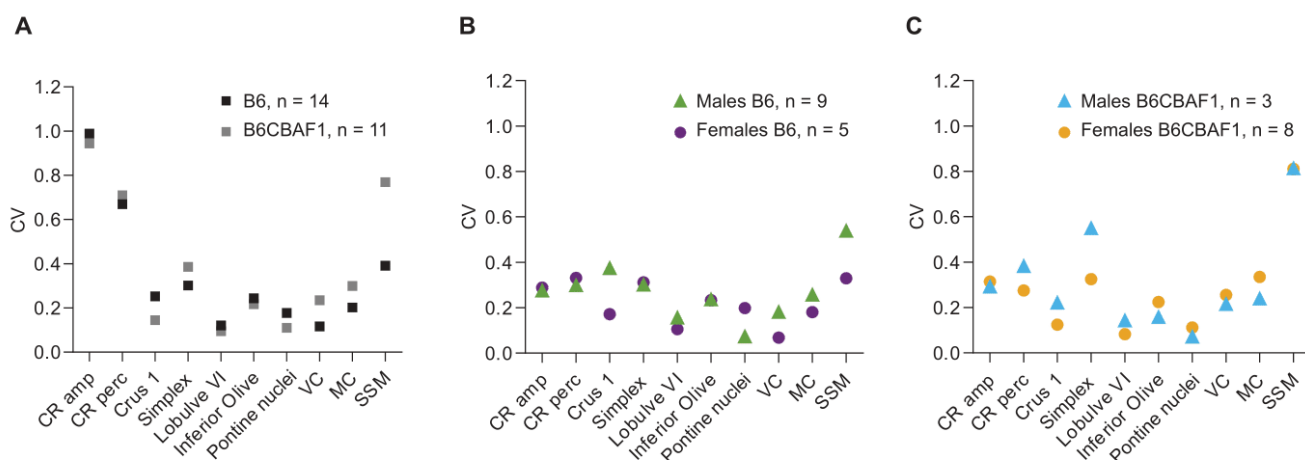


**Figure 5:** Correlation between learning scores and *C-fos* expression is consistent in B6CBAF1 mice. **A)** CR percentage in CS only trials over training sessions. Yellow: females (n = 9), cyan: males (n = 7). Shaded area: sem. **B)** CR amplitude in CS only trials over training sessions. Shaded area: sem **C)** C-FOS positive cells in the lobule VI. **D)** Cerebellar areas with significant positive correlation between C-FOS positive cell density and CR amplitude (crus 1: tau = 0.82,  $p = 0.0001$ , simplex: tau = 0.7,  $p = 0.005$ , lobule VI: tau = 0.75,  $p = 0.0007$ ). **E)** C-FOS positive cells in the inferior olive. **F)** Brainstem areas with significant positive correlation between C-FOS positive cell density and CR amplitude (inferior olive: tau = 0.85,  $p = 0.0004$ , pontine nuclei: tau = 0.78,  $p = 0.0003$ ). **G)** C-FOS positive cells in the visual cortex. **H)** Cortical areas with significant positive correlation between C-FOS positive cell density and CR amplitude (visual cortex: tau = 0.64,  $p = 0.0057$ , motor cortex: tau = 0.75,  $p = 0.0008$ , somatosensory cortex: tau = 0.6,  $p = 0.009$ ).

### 219 Variability between sexes and strains

220 To further understand inter-strain and inter-sex variability in our dataset, we calculated the coefficient of  
 221 variance (CV, standard deviation/mean) for each of the variables that we quantify in both B6 and B6CBAF1 mice.  
 222 We selected the 14 learners (CR amplitude on session 5 > 0.4) B6 mice (n = 5 males, 9 females) and the 11 learners

223 B6CBAF1 mice (n = 3 males, 8 females) and grouped them by strain and sex (**Fig. 6**). For each group, we calculated  
 224 the CV for the common variables acquired and previously reported, which can be grouped in two main categories:  
 225 eyeblink performance and *C-fos* expression. Eyeblink performance includes CR amplitude and percentage. *C-fos*  
 226 expression includes the density of C-FOS positive cells in the brain areas where we have found a positive significant  
 227 correlation across both strains: crus 1, simplex, lobule VI, inferior olive, pontine nuclei, and the visual, motor and  
 228 somatosensory cortices. When comparing strains, we observed that the variances for each variable were similar,  
 229 with the exception of the somatosensory cortex, where B6CBAF1 mice seem to be more variable compared to B6  
 230 (**Fig. 6A**). B6 female and male mice had similar CVs for most of the variables, although in crus 1 and the  
 231 somatosensory cortex males seem to have a slightly higher CV (**Fig. 6B**). However, this could be due to the  
 232 difference in sample size. We observed something similar between B6CBAF1 female and male mice; males showed  
 233 slightly higher CV in C-FOS density in the simplex (**Fig. 6C**). Additionally, B6CBAF1 mice had the highest CV in  
 234 the somatosensory cortex.



235

**Figure 6:** Strain and sex variability. Learners were selected if CR amplitude on session 5 > 0.4. CV = STD/mean. **A)** For strains: B6, n = 14, B6CBAF1, n = 11. **B)** For B6 mice: males B6, n = 9, females B6, n = 5. **C)** For B6CBAF1 mice: males, n = 3, females, n = 8. VC: visual cortex; MC: motor cortex; SSM: somatosensory cortex; CV: Coefficients of variation.

236

237



## 238 **Discussion**

239 Understanding behavioral variability in the context of neuroscience research is a challenge. We are still far  
240 from fully comprehending how factors like sex and strain give rise to differences in behavior.

241 Here we addressed this question by making use of a well-known learning paradigm to study behavioral  
242 variability. We found that B6 female and male mice showed comparable variance in delay eyeblink conditioning  
243 and locomotion while being head-fixed on a rotating wheel. The variance within these behaviors was not different  
244 between sexes, yet females reached higher learning scores and running speeds within five days of training.  
245 Importantly, we found a robust correlation between learning scores and running speed which is consistent across  
246 sexes. In a similar way, we found that enriched *C-fos* expression across several brain areas positively correlates  
247 with learning, which suggests the involvement of these regions in eyeblink conditioning. Finally, we observed  
248 similar results in a hybrid mouse strain (B6CBAF1).

249  
250 *Sex, strain and behavior: comparable variability but difference in performance*

251 Opposed to what is sometimes assumed in behavioral science, we observed that sexes show comparable  
252 variability. However, we found differences in performance during eyeblink conditioning and locomotion. Common  
253 behaviors like duration of running vary between female and male mice in the wild (Lightfoot et al., 2004; Goh &  
254 Ladiges, 2015). Behaviors widely assessed in research such as fear conditioning and navigation on the Morris water  
255 maze also show differences depending on sex (Roof & Stein, 1999; Keeley et al., 2013; Yang et al., 2013; Gruene,  
256 Flick, et al., 2015). In the context of cerebellar-dependent learning, evidence shows that estradiol increases the  
257 density of parallel fiber to Purkinje cell synapse and induces long-term potentiation, which improves memory  
258 formation (Andreescu et al., 2007). In trace eyeblink conditioning, both sexes reach similar learning scores but  
259 females show significantly higher CR percentage compared to males in the first five days of learning, which is in  
260 line with our findings (Rapp et al., 2021). Considering that adapting motor reflexes is a highly conserved behavior,  
261 it is logical that both sexes reach similar asymptotic learning scores in longer paradigms. However, these findings  
262 together with our results suggest that females exhibit faster learning rates during the first stages of learning.

263 Therefore, we postulate that using females could reduce the training time to achieve desired scores, which  
264 could be advantageous for certain experiments, particularly time-sensitive ones, such as calcium imaging or  
265 electrophysiological measurements. In addition, our results show that male and female mice have similar variability,  
266 which indicates that females can be included in studies without taking into account the estrous cycle phase. In  
267 general, utilizing both sexes would reduce the overall number of animals used in research, and increase the relevance  
268 and generalization of scientific findings.

269 A common experimental setting in neuroscience involves head-fixing awake mice and placing them on a  
270 freely moving wheel. A recent study investigated sex differences in head-fixed running behavior and found that  
271 female mice ran forward naturally within the first two days, while males took seven days to progressively learn to  
272 only run forward (Prawira, 2019). In our experiments, the differences in learning scores between sexes were strongly  
273 correlated to the changes in locomotor activity on the wheel. Our results show that the previously reported  
274 correlation between imposed locomotor activity and learning scores (Albergaria et al., 2018) persists when mice  
275 can initiate locomotion voluntarily. This suggests that spontaneous locomotion might facilitate associative learning  
276 and could be predictive of learning scores.

277 Finally, we have found that, besides moving slower, males tended to have a tilted position on the wheel  
278 compared to females. These differences in body position could be partially caused by differences in stress levels  
279 that, at the same time, could affect learning rates. It is known that stress plays an important role in modulating neural  
280 activity in the hippocampus. Corticosterone - among other stress hormones – increases CA1/CA3 firing rates shortly  
281 after a stressful period and induces molecular cascades that enhance calcium influx, which disrupts hippocampal  
282 function (Joëls, 2009). Similar mechanisms have been described in the cerebellum; calcium-based excitability in  
283 the DCN is altered in animals with higher levels of corticosterone evoked by shipping stress (Schneider et al., 2013).

284

### 285 *Associative learning networks*

286 Our results show that the expression of *C-fos* in the cerebellar cortex, following delay eyeblink  
287 conditioning, is localized to the granule cell layer. This is expected, given that multiple forms of plasticity have  
288 been shown within the synapses in this layer. For example, the mossy fiber-granule cell synapse undergoes both

289 long-term potentiation and long-term depression (Gao et al., 2012), and evidence has shown that granule cell activity  
290 adapts over time during eyeblink conditioning (Giovannucci et al., 2017) and other types of learning (Knogler et  
291 al., 2017; Wagner et al., 2017). In addition, induction of LTP by theta-burst stimulation in acute cerebellar slices  
292 activates cAMP-responsive element binding protein (CREB) cascade which, in turn, activates *C-fos* expression  
293 (Gandolfi et al., 2017). Our results are consistent with these findings and, overall, they provide evidence on how  
294 plasticity, at the input level in the cerebellar cortex, can evoke transcriptional processes that contribute to learning  
295 consolidation. The strongest correlations between *C-fos* expression and CR amplitude within the cerebellum were  
296 observed in simplex, lobule VI, and crus 1, which is consistent with the “eyeblink region”, but expands beyond the  
297 small area usually recorded using electrophysiological approaches (Heiney et al., 2014a; ten Brinke et al., 2015).  
298 Strong *C-fos* expression in crus 1 supports our previous findings showing the importance of this lobule in eyeblink  
299 conditioning (Badura et al., 2018).

300         Outside of the cerebellum, we identified several brain areas that could play a role in eyeblink conditioning.  
301 At the brainstem level, we found a relation between high learning scores and *C-fos* expression in the pons, inferior  
302 olive, red nucleus and facial nucleus. High activity in the red nucleus and facial nucleus is to be expected, given  
303 that these two nuclei, together with the oculomotor nucleus, execute the blink. The inferior olive and the pontine  
304 nuclei relay the US and CS information to the cerebellar cortex, respectively. During early training sessions, the US  
305 is a highly aversive stimulus, which makes it comparatively more salient than the CS signal. Hence, one would  
306 expect increased activity in the pons relative to the inferior olive. However, in later learning stages (when animals  
307 have consolidated the association), the CS is predictive of the US, which would increase the activity in the inferior  
308 olive relative to the pons. We found a correlation between learning scores and C-FOS positive cells in both the pons  
309 and the inferior olive, which could indicate an intermediate stage of learning, where animals have learned the  
310 association but the US information is still relevant.

311         Moreover, we found higher *C-fos* expression in the visual, motor and somatosensory cortices in mice with  
312 higher learning scores. Processing in these cortices could facilitate the CS to become more salient and ultimately  
313 predict the US. The somatosensory cortex projects to the lateral amygdala which, in turn, projects to the central  
314 amygdala, to ultimately contact the pons. The high *C-fos* expression found in the amygdala points towards a two

315 stage conditioning model; where the amygdala would have an initial role with arousal as a salient feature, and a  
316 second phase where the cerebellum would take over to form precisely-timed CRs (Boele et al., 2010). In the motor  
317 cortex, higher C-FOS levels in high performing mice might be due to locomotor activity rather than learning itself.  
318 However, as mentioned above, this could play a role in learning either by directly affecting cerebellar input or  
319 indirectly as arousal.

320 Finally, we found an enrichment of *C-fos* expression in upper cortical layers (II, III and IV), especially in  
321 the visual and somatosensory cortices. The principal excitatory neurons in layers II/III have large axons that project  
322 to other telencephalic areas, such as the cortex and the striatum (Adesnik and Naka, 2018), while neurons in layer  
323 IV form loops within the layer and connect to layers II/III and VI (Scala et al., 2019). Layers VI and VII are thought  
324 to be the main outputs of the cerebral cortex, connecting to multiple subcortical areas and the thalamus, respectively  
325 (Harris and Shepherd, 2015). The higher C-FOS density in upper cortical layers indicates higher neuronal activity.  
326 This could reflect feedforward loops within neuronal populations and translaminar connectivity that could reinforce  
327 learning. However, further research is needed to determine the identity of these neurons.

328 Together, these findings give us a better understanding of the networks underlying eyeblink conditioning  
329 and provide candidate brain areas to be further researched in the context of associative learning.

330  
331  
332

## 333 **Materials and Methods**

### 334 *Animals*

335 All experiments were performed in accordance with the European Communities Council Directive. All  
336 animal protocols were approved by the Dutch National Experimental Animal Committee (DEC). C57BL/6J mice  
337 were ordered from Charles River (n = 16 males; n = 16 females), and B6CBAF1 mice from Janvier (n = 7 males; n  
338 = 9 females). Mice were group-housed and kept on a 12-hour light-dark cycle with ad libitum food and water. All  
339 procedures were performed in male and female mice approximately 8-12 weeks of age.

### 340 *Eyeblink pedestal placement surgery*

341 Mice were anesthetized with isoflurane and oxygen (4% isoflurane for induction and 2-2.5% for  
342 maintenance). Body temperature was monitored during the procedure and maintained at 37°C. Animals were fixed  
343 in a stereotaxic device (Model 963, David Kopf Instruments, Tujunga CA, USA). The surgery followed previously  
344 described standard procedures for pedestal placement (Gao et al., 2016; ten Brinke et al., 2017). In short, the hair  
345 on top of the head was shaved, betadine and lidocaine were applied on the skin and an incision was done in the  
346 scalp to expose the skull. The tissue on top of the skull was removed and the skull was kept dry before applying  
347 Optibond™ prime adhesive (Kerr, Bioggio, Switzerland). A pedestal equipped with a magnet (weight ~1g), was  
348 placed on top with Charisma® (Heraeus Kulzer, Armonk NY, USA), which was hardened with UV light. Rymadil  
349 was injected subcutaneously (5mg per kg). Mice were left under a heating lamp for recovery for at least 3 hours.  
350 Mice were given 3-4 resting days before starting experiments.

### 351 *Eyeblink conditioning*

352 Mice were habituated to the set-up (head fixed to a bar suspended over a cylindrical treadmill in a sound  
353 and light isolating chamber) for 5 days with increasing exposure (15, 15, 30, 45 and 60 min). Training started after  
354 two rest days. Twenty-eight 57BL/6 mice (n = 16 males; n = 16 females), and 16 B6CBAF1 mice (n = 7 males; n  
355 = 9 females) were trained using the standard eyeblink protocol (Brinke et al., 2015, Koekkoek et al., 2002). Ten  
356 CS-only trials of 30 ms with an inter-trial interval (ITI) of  $10 \pm 2$  s were presented before the first training session  
357 to acquire a baseline measurement. Mice were next trained for 5 consecutive days. Each session consisted of 20

358 blocks of 12 trials each (1 US only, 11 paired and 1 CS only) with an ITI of  $10 \pm 2$  s. The CS was a 270 ms blue  
359 LED light ( $\sim 450$  nm) placed 7 cm in front of the mouse. The US was a 30 ms corneal air puff co-terminating with  
360 the CS. The puffer was controlled by a VHS P/P solenoid valve set at 30 psi (Lohm rate, 4750 Lohms; Internal  
361 volume, 30  $\mu$ L, The Lee Company®, Westbrook, US) and delivered via a 27.5 mm gauge needle at 5 mm from the  
362 center of the left cornea. The inter-stimulus interval was 250 ms. Eyelid movements were recorded with a camera  
363 (Baseler aceA640) at 250 frames/s. 4 C57BL/6 mice ( $n = 2$  males;  $n = 2$  females), were trained using a  
364 pseudoconditioning protocol. Pseudoconditioning protocol consisted of 20 blocks of 12 trials each (1 puff only, 12  
365 LED only) with an ITI of  $10 \pm 2$  s. The puff and LED stimulus had the same characteristics as in the conditioning  
366 protocol. Data was analyzed with a custom written MATLAB code as previously described (Giovannucci et al.,  
367 2017; Badura et al., 2018). Traces were normalized within each session to the UR max amplitude. The CR detection  
368 window was set to 650-730 ms and CRs were only classified as such when the amplitude was equal or higher than  
369 5% of the UR median. The CR percentage was calculated as the number of counted CRs (equal or higher than 5%  
370 of the UR median) divided by the total CS trials per session.

### 371 *Locomotion*

372 An infrared camera (ELP 1080P) (sampling frequency 60 frames/s) was placed in each of the eyeblink  
373 boxes and connected to an external computer (independent from the eyeblink system). The cameras were positioned  
374 at the right back corner of the chamber on top of a magnet tripod attached to a custom-made metal block which  
375 allowed stable fixation. The recording angle was standardized by selecting the same reference in the field of view  
376 of each camera. Simultaneous video acquisition from the three cameras was performed in Ipi Recorder software  
377 (<http://ipisoft.com/download/>). Body movement recording was parallel to eyelid recording during the training  
378 sessions. The output videos (.avi format) from each mouse and session were approximately 35 min (corresponding  
379 to the length of an eyeblink session).

### 380 *Locomotion analysis*

381 We used DeepLabCut (DLC) to track body parts from videos (Mathis et al., 2018) (**Fig. 2**). We extracted  
382 40 frames of 4 different videos from two males and two females (total of 160 frames). Next, frames were manually

383 labeled with 5 body parts (tail base, hip, knee, right back paw and nose). These frames were used for training the  
384 pre-trained deep neural network ResNet50 (He et al., 2016; Insafutdinov et al., 2016). Evaluation of the network  
385 was done to confirm a low error in pixels between labeled frames and predictions. Video analysis was done by using  
386 the trained network to get the locations of body parts from all mice and sessions (16 mice x 5 sessions = 80 videos).  
387 DLC output is a matrix with x and y positions in pixels and the likelihood of this position for each body part. We  
388 used this matrix to calculate distance covered and speed per body part with a custom written code  
389 ([https://github.com/BaduraLab/DLC\\_analysis](https://github.com/BaduraLab/DLC_analysis)). After confirming normal distribution of the spatial coordinates per  
390 body part over training sessions, we performed the Grubbs's test for outlier removal to discard possible tracking  
391 errors.

#### 392 *Tissue processing*

393 Mice were anesthetized with 0.2 ml pentobarbital (60 mg/ml) and perfused with 0.9% NaCl followed by  
394 4% paraformaldehyde (PFA). Given the peak time expression of *C-fos* (Chung, 2015), animals were perfused 90  
395 minutes after finishing the last training session. Brains were dissected from the skull and stored in 4% PFA at room  
396 temperature (rT) for 1.5 hours. They were next changed to a 10% sucrose solution and left overnight at 4°C. Brains  
397 were embedded in 12% gelatin and 10% sucrose and left in a solution with 30% sucrose and 4% PFA in PBS at rT  
398 for 1.5 hours. Next, they were transferred to a 30% sucrose solution in 0.1 M PB and kept at 4°C. Whole brains  
399 were sliced at 50  $\mu$ m with a microtome and slices were kept in 0.1 M PB.

#### 400 *Immunostaining and Imaging*

401 Sections were incubated in blocking solution (10% NHS, 0.5% Triton in PBS) for an hour at rT. After  
402 rinsing, sections were incubated for 48 hours at 4°C on a shaker in primary antibody solution with 2% NHS (1:2000  
403 Rabbit anti-C-FOS, ab208942, Abcam; 1:1000 Rat anti-Ctip2, ab18465, Abcam; 1:1000 Rabbit anti-GABAalpha6,  
404 G5555, Sigma-Aldrich; 1:1000 Rabbit anti-Cux1, (Ellis et al., 2001)). After rinsing, sections were incubated for 2  
405 hours at rT on a shaker with secondary antibody (1:500 Donkey anti-rabbit A594, 711-585-152, Jackson; 1:500  
406 Donkey anti-Rabbit A488, 711-545-152, Jackson; 1:500 Donkey anti-rabbit Cy5, 711-175-152, Jackson; Donkey

407 anti-rat Cy3, 712-165-150, Jackson). Sections were counterstained with DAPI. Finally, sections were rinsed in 0.1  
408 PB, placed with chromulin on coverslips and mounted on slide glasses with Mowiol.

409 Sections were imaged with a Zeiss AxioImager 2 (Carl Zeiss, Jena, Germany) at 10x. A DsRed filter and  
410 an exposure time of 300 ms was used for the Alexa 595 channel (C-FOS). The DAPI channel was scanned at 20 ms  
411 or 30 ms exposure time. Tile scans were taken from whole brain slices. We processed half the sections obtained  
412 from slicing, hence, the distance between tile scan images was 100  $\mu$ m. High resolution images were taken with a  
413 LSM 700 confocal microscope (Carl Zeiss, Jena, Germany).

#### 414 *Image analysis*

415 We developed an image analysis workflow for brain region identification and quantification of C-FOS  
416 positive neurons following eyeblink conditioning (**Supp. Fig. 1**) (<https://github.com/BaduraLab/cell-counting>). The  
417 workflow combines Fiji and a SHARP-Track, a software written in MATLAB initially developed to localize brain  
418 regions traversed by electrode tracks (Shamash et al., 2018) ([https://github.com/cortex-](https://github.com/cortex-lab/allenCCF/tree/master/SHARP-Track)  
419 [lab/allenCCF/tree/master/SHARP-Track](https://github.com/cortex-lab/allenCCF/tree/master/SHARP-Track)). Brain slices were preprocessed (rotating, cropping and scaling) with a  
420 custom written macro in Fiji (Schindelin et al., 2012). Next, slices were registered to the Allen Brain Atlas using  
421 the SHARP-Track user interface. Segmentation was performed on the registered slices in Fiji. Given the  
422 characteristic C-FOS staining pattern in the cerebellar granule layer (**Fig 3. A**), we used different thresholding  
423 algorithms for the cerebellum and for the rest of the brain. Following that, automated cell counting of C-FOS  
424 positive neurons was performed with a custom written macro in Fiji (cerebellum - circularity: 0.5-1, size: 0-20  
425 pixels, rest of the brain - circularity: 0.7-1, size: 0-40 pixels) to get the X and Y coordinates of every detected cell.  
426 The output matrix of coordinates was used to create a ROI array per slice in SHARP-Track. This step allows one to  
427 one matching between the ROI array and the previously registered slice. Finally, the reference-space locations and  
428 brain regions of each neuron were obtained by overlapping the registration array with the ROI array. ROI counts  
429 were normalized by brain region surface following the hierarchical structure of the Allen Brain Atlas. The surface  
430 of each brain areas was calculated per slice and cell density was defined as ROI counts/surface.



431 *Statistics*

432 Statistics were performed in MATLAB and GraphPad Prism 6. Data is reported as mean  $\pm$  std or sem.

433 Normality was tested and accepted for both eyeblink CR amplitudes and for speed of the right back paw. The

434 corresponding statistical test for the  $p$  values reported are specified in Results. Time data (training sessions) was

435 analyzed using two-way repeated measures ANOVA for sex and session. Sex effect is reported in Results, session

436 effect is significant in all groups (indicating learning through time) and interaction is reported if significant. For

437 Kendalls's correlation on C-FOS data, we report Tau and  $p$  values.

438

439 **Acknowledgments**

440 We thank Roxanne ter Haar, Elize D. Haasdijk and Stephanie Dijkhuizen for their help with experiments. This work  
441 was supported by Dutch Research Council (Vidi/ZonMw/917.18.380,2018).

442

443

444 **Competing interests**

445 The authors declare no competing interests.

446

447 **References**

- 448 Adesnik H, Naka A (2018) Cracking the Function of Layers in the Sensory Cortex. *Neuron* 100:1028–1043  
449 <https://doi.org/10.1016/j.neuron.2018.10.032>.
- 450 Åhlgren J, Voikar V (2019) Experiments done in Black-6 mice: what does it mean? *Lab Anim (NY)* 48:171–180.
- 451 Albergaria C, Silva NT, Pritchett DL, Carey MR (2018) Locomotor activity modulates associative learning in  
452 mouse cerebellum. *Nat Neurosci* 21:725–735 <http://dx.doi.org/10.1038/s41593-018-0129-x>.
- 453 Andreescu CE, Milojkovic BA, Haasdijk ED, Kramer P, De Jong FH, Krust A, De Zeeuw CI, De Jeu MTG  
454 (2007) Estradiol improves cerebellar memory formation by activating estrogen receptor  $\beta$ . *J Neurosci*  
455 27:10832–10839.
- 456 Arnold MA, Newland MC (2018) Variable behavior and repeated learning in two mouse strains: Developmental  
457 and genetic contributions. *Behav Processes* 157:509–518 <https://doi.org/10.1016/j.beproc.2018.06.007>.
- 458 Badura A, Verpeut JL, Metzger JW, Pereira TD, Pisano TJ, Deverett B, Bakshinskaya DE, Wang SSH (2018)  
459 Normal cognitive and social development require posterior cerebellar activity. *Elife* 7:1–36.
- 460 Becker JB, Prendergast BJ, Liang JW (2016) Female rats are not more variable than male rats: A meta-analysis of  
461 neuroscience studies. *Biol Sex Differ* 7:1–7 <http://dx.doi.org/10.1186/s13293-016-0087-5>.
- 462 Bernstein HL, Lu YL, Botterill JJ, Scharfman HE (2019) Novelty and novel objects increase c-fos  
463 immunoreactivity in mossy cells in the mouse dentate gyrus. *Neural Plast* 2019.
- 464 Bettis TJ, Jacobs LF (2009) Sex-specific strategies in spatial orientation in C57BL/6J mice. *Behav Processes*  
465 82:249–255.
- 466 Boele HJ, Koekkoek SKE, De Zeeuw CI (2010) Cerebellar and extracerebellar involvement in mouse eyeblink  
467 conditioning: The ACDC model. *Front Cell Neurosci* 3:1–13.
- 468 Bucán M, Abel T (2002) The mouse: genetics meets behavior. *Nat Rev Genet*  
469 <https://www.nature.com/articles/nrg728?draft=marketing>.
- 470 Chung L (2015) A Brief Introduction to the Transduction of Neural Activity into Fos Signal. *Dev Reprod* 19:61–  
471 67.
- 472 D’Angelo E, Galliano E, De Zeeuw CI (2016) Editorial: The olivo-cerebellar system. *Front Neural Circuits*  
473 9:2015–2017.
- 474 Ellis T, Gambardella L, Horcher M, Tschanz S, Capol J, Bertram P, Jochum W, Barrandon Y, Busslinger M  
475 (2001) The transcriptional repressor CDP (Cutl1) is essential for epithelial cell differentiation of the lung  
476 and the hair follicle. *Genes Dev* 15:2307–2319.
- 477 Erway LC, Shiau YW, Davis RR, Krieg EF (1996) Genetics of age-related hearing loss in mice. III. Susceptibility  
478 of inbred and F1 hybrid strains to noise-induced hearing loss. *Hear Res* 93:181–187.

- 479 Faure A, Pittaras E, Nosjean A, Chabout J, Cressant A, Granon S (2017) Social behaviors and acoustic  
480 vocalizations in different strains of mice. *Behav Brain Res* 320:383–390  
481 <http://dx.doi.org/10.1016/j.bbr.2016.11.003>.
- 482 Festing MFW (1999) Warning: The use of heterogeneous mice may seriously damage your research. *Neurobiol*  
483 *Aging* 20:237–244.
- 484 Fonnesu M, Kuczewski N (2019) Doubts on the efficacy of outliers correction methods.
- 485 Gallo FT, Katche C, Morici JF, Medina JH, Weisstaub N V. (2018) Immediate early genes, memory and  
486 psychiatric disorders: Focus on c-Fos, Egr1 and Arc. *Front Behav Neurosci* 12:1–16.
- 487 Gandolfi D, Cerri S, Mapelli J, Polimeni M, Tritto S, Fuzzati-Armentero MT, Bigiani A, Blandini F, Mapelli L,  
488 D’Angelo E (2017) Activation of the CREB/c-Fos pathway during long-term synaptic plasticity in the  
489 cerebellum granular layer. *Front Cell Neurosci* 11:1–13.
- 490 Gao Z, Proietti-Onori M, Lin Z, ten Brinke MM, Boele HJ, Potters JW, Ruigrok TJH, Hoebeek FE, De Zeeuw CI  
491 (2016) Excitatory Cerebellar Nucleocortical Circuit Provides Internal Amplification during Associative  
492 Conditioning. *Neuron* 89:645–657.
- 493 Gao Z, Van Beugen BJ, De Zeeuw CI (2012) Distributed synergistic plasticity and cerebellar learning. *Nat Rev*  
494 *Neurosci* 13:619–635.
- 495 Giovannucci A, Badura A, Deverett B, Najafi F, Pereira TD, Gao Z, Ozden I, Kloth AD, Pnevmatikakis E,  
496 Paninski L, De Zeeuw CI, Medina JF, Wang SSH (2017) Cerebellar granule cells acquire a widespread  
497 predictive feedback signal during motor learning. *Nat Neurosci* 20:727–734.
- 498 Gormezano I, Schneiderman N, Deaux E, Fuentes I (1962) Nictitating membrane: Classical conditioning and  
499 extinction in the albino rabbit. *Science* (80- ) 138:33–34.
- 500 Grissom NM, McKee SE, Schoch H, Bowman N, Havekes R, O’Brien WT, Mahrt E, Siegel S, Commons K,  
501 Portfors C, Nickl-Jockschat T, Reyes TM, Abel T (2018) Male-specific deficits in natural reward learning in  
502 a mouse model of neurodevelopmental disorders. *Mol Psychiatry* 23:544–555.
- 503 Harris KD, Shepherd GMG (2015) The neocortical circuit: Themes and variations. *Nat Neurosci* 18:170–181.
- 504 He K, Zhang X, Ren S, Sun J (2016) Deep residual learning for image recognition. *Proc IEEE Comput Soc Conf*  
505 *Comput Vis Pattern Recognit* 2016-Decem:770–778.
- 506 Heiney SA, Kim J, Augustine GJ, Medina JF (2014a) Precise control of movement kinematics by optogenetic  
507 inhibition of Purkinje cell activity. *J Neurosci* 34:2321–2330.
- 508 Heiney SA, Wohl MP, Chettih SN, Ruffolo LI, Medina JF (2014b) Cerebellar-dependent expression of motor  
509 learning during eyeblink conditioning in head-fixed mice. *J Neurosci* 34:14845–14853.
- 510 Hendershott TR, Cronin ME, Langella S, McGuinness PS, Basu AC (2016) Effects of environmental enrichment  
511 on anxiety-like behavior, sociability, sensory gating, and spatial learning in male and female C57BL/6J

- 512 mice. *Behav Brain Res* 314:215–225 <http://dx.doi.org/10.1016/j.bbr.2016.08.004>.
- 513 Hoogland TM, De Gruijl JR, Witter L, Canto CB, De Zeeuw CI (2015) Role of synchronous activation of  
514 cerebellar purkinje cell ensembles in multi-joint movement control. *Curr Biol* 25:1157–1165  
515 <http://dx.doi.org/10.1016/j.cub.2015.03.009>.
- 516 Insafutdinov E, Pishchulin L, Andres B, Andriluka M, Schiele B (2016) Deepercut: A deeper, stronger, and faster  
517 multi-person pose estimation model. *Lect Notes Comput Sci (including Subser Lect Notes Artif Intell Lect*  
518 *Notes Bioinformatics)* 9910 LNCS:34–50.
- 519 Joëls M (2009) Stress, the hippocampus, and epilepsy. *Epilepsia* 50:586–597.
- 520 Joo JY, Schaukowitz K, Farbiak L, Kilaru G, Kim TK (2015) Stimulus-specific combinatorial functionality of  
521 neuronal c-fos enhancers. *Nat Neurosci* 19:75–83.
- 522 Knogler LD, Markov DA, Dragomir EI, Štih V, Portugues R (2017) Sensorimotor Representations in Cerebellar  
523 Granule Cells in Larval Zebrafish Are Dense, Spatially Organized, and Non-temporally Patterned. *Curr Biol*  
524 27:1288–1302.
- 525 Konhilas JP, Maass AH, Luckey SW, Stauffer BL, Olson EN, Leinwand LA (2004) Sex modifies exercise and  
526 cardiac adaptation in mice. *Am J Physiol - Hear Circ Physiol* 287:2768–2776.
- 527 Kratochwil CF, Maheshwari U, Rijli FM (2017) The long journey of pontine nuclei neurons: From rhombic lip to  
528 cortico-ponto-cerebellar circuitry. *Front Neural Circuits* 11:1–19.
- 529 Leung C, Jia Z (2016) Mouse genetic models of human brain disorders. *Front Genet* 7:1–20.
- 530 Löwgren K, Bååth R, Rasmussen A, Boele HJ, Koekkoek SKE, De Zeeuw CI, Hesslow G (2017) Performance in  
531 eyeblink conditioning is age and sex dependent. *PLoS One* 12:1–15.
- 532 Mathis A, Mamidanna P, Cury KM, Abe T, Murthy VN, Mathis MW, Bethge M (2018) DeepLabCut: markerless  
533 pose estimation of user-defined body parts with deep learning. *Nat Neurosci* 21:1281–1289  
534 <http://dx.doi.org/10.1038/s41593-018-0209-y>.
- 535 McGinley MJ, Vinck M, Reimer J, Batista-Brito R, Zagha E, Cadwell CR, Tolias AS, Cardin JA, McCormick DA  
536 (2015) Waking State: Rapid Variations Modulate Neural and Behavioral Responses. *Neuron* 87:1143–1161  
537 <http://dx.doi.org/10.1016/j.neuron.2015.09.012>.
- 538 Meziane H, Ouagazzal AM, Aubert L, Wietrzyk M, Krezel W (2007) Estrous cycle effects on behavior of  
539 C57BL/6J and BALB/cByJ female mice: Implications for phenotyping strategies. *Genes, Brain Behav*  
540 6:192–200.
- 541 Milon B, Mitra S, Song Y, Margulies Z, Casserly R, Drake V, Mong JA, Depireux DA, Hertzano R (2018) The  
542 impact of biological sex on the response to noise and otoprotective therapies against acoustic injury in mice.  
543 *Biol Sex Differ* 9:1–14.
- 544 Ohlemiller KK (2019) Mouse methods and models for studies in hearing. *J Acoust Soc Am* 146:3668–3680.

- 545 Osborne JW, Overbay A (2004) The power of outliers (and why researchers should ALWAYS check for them).  
546 Pract Assessment, Res Eval 9. <https://doi.org/10.7275/qf69-7k43>  
547
- 548 Ozden I, Dombeck DA, Hoogland TM, Tank DW, Wang SSH (2012) Widespread state-dependent shifts in  
549 cerebellar activity in locomoting mice. PLoS One 7.
- 550 Pfaff D (2001) Precision in mouse behavior genetics. Proc Natl Acad Sci U S A 98:5957–5960.
- 551 Powell K, Mathy A, Duguid I, Häusser M (2015) Synaptic representation of locomotion in single cerebellar  
552 granule cells. Elife 4:1–18.
- 553 Prawira Y (2019) Sex differences in head-fixed running behavior. SSRN Electron J 5:1–19.
- 554 Rapp AP, Weiss C, Matthew Oh M, Disterhoft JF (2021) Intact female mice acquire trace eyeblink conditioning  
555 faster than male and ovariectomized female mice. eNeuro 8:1–9.
- 556 Rivera J, Tessarollo L (2008) Genetic Background and the Dilemma of Translating Mouse Studies to Humans.  
557 Immunity 28:1–4.
- 558 Rousselet GA, Pernet CR (2012) Improving standards in brain-behavior correlation analyses. Front Hum Neurosci  
559 6.
- 560 Ruigrok TJH (2011) Ins and outs of cerebellar modules. Cerebellum 10:464–474.
- 561 Scala F, Kobak D, Shan S, Bernaerts Y, Laternus S, Cadwell CR, Hartmanis L, Froudarakis E, Castro JR, Tan  
562 ZH, Papadopoulos S, Patel SS, Sandberg R, Berens P, Jiang X, Tolias AS (2019) Layer 4 of mouse  
563 neocortex differs in cell types and circuit organization between sensory areas. Nat Commun 10:1–12  
564 <http://dx.doi.org/10.1038/s41467-019-12058-z>.
- 565 Schindelin J, Arganda-Carreras I, Frise E, Kaynig V, Longair M, Pietzsch T, Preibisch S, Rueden C, Saalfeld S,  
566 Schmid B, Tinevez JY, White DJ, Hartenstein V, Eliceiri K, Tomancak P, Cardona A (2012) Fiji: An open-  
567 source platform for biological-image analysis. Nat Methods 9:676–682.
- 568 Schneider ER, Civillico EF, Wang SSH (2013) Calcium-based dendritic excitability and its regulation in the deep  
569 cerebellar nuclei. J Neurophysiol 109:2282–2292.
- 570 Schreurs BG, Smith-Bell C, Burhans LB (2018) Sex differences in a rabbit eyeblink conditioning model of PTSD.  
571 Neurobiol Learn Mem 155:519–527.
- 572 Shamash P, Carandini M, Harris K, Steinmetz N (2018) A tool for analyzing electrode tracks from slice histology.  
573 <http://dx.doi.org/10.1101/447995>.
- 574 Simpson J, Kelly JP (2012) An investigation of whether there are sex differences in certain behavioural and  
575 neurochemical parameters in the rat. Behav Brain Res 229:289–300  
576 <http://dx.doi.org/10.1016/j.bbr.2011.12.036>.
- 577 Sittig LJ, Carbonetto P, Engel KA, Krauss KS, Barrios-Camacho CM, Palmer AA (2016) Genetic Background

578 Limits Generalizability of Genotype-Phenotype Relationships. *Neuron* 91:1253–1259  
579 <http://dx.doi.org/10.1016/j.neuron.2016.08.013>.

580 ten Brinke MM, Boele HJ, Spanke JK, Potters JW, Kornysheva K, Wulff P, Ijpelaar ACHG, Koekkoek SKE, De  
581 Zeeuw CI (2015) Evolving Models of Pavlovian Conditioning: Cerebellar Cortical Dynamics in Awake  
582 Behaving Mice. *Cell Rep* 13:1977–1988 <http://dx.doi.org/10.1016/j.celrep.2015.10.057>.

583 ten Brinke MM, Heiney SA, Wang X, Proietti-Onori M, Boele HJ, Bakermans J, Medina JF, Gao Z, De Zeeuw CI  
584 (2017) Dynamic modulation of activity in cerebellar nuclei neurons during pavlovian eyeblink conditioning  
585 in mice. *Elife* 6:1–27.

586 Tye KM, Prakash R, Kim SY, Fenno LE, Grosenick L, Zarabi H, Thompson KR, Gradinaru V, Ramakrishnan C,  
587 Deisseroth K (2011) Amygdala circuitry mediating reversible and bidirectional control of anxiety. *Nature*  
588 471:358–362.

589 Vinck M, Batista-Brito R, Knoblich U, Cardin JA (2015) Arousal and Locomotion Make Distinct Contributions to  
590 Cortical Activity Patterns and Visual Encoding. *Neuron* 86:740–754  
591 <http://dx.doi.org/10.1016/j.neuron.2015.03.028>.

592 Wagner MJ, Kim TH, Savall J, Schnitzer MJ, Luo L (2017) Cerebellar granule cells encode the expectation of  
593 reward. *Nature* 544:96–100 <http://dx.doi.org/10.1038/nature21726>.

594 Williamson RS, Hancock KE, Shinn-Cunningham BG, Polley DB (2015) Locomotion and Task Demands  
595 Differentially Modulate Thalamic Audiovisual Processing during Active Search. *Curr Biol* 25:1885–1891  
596 <http://dx.doi.org/10.1016/j.cub.2015.05.045>.

597 Wolfer DP, Crusio WE, Lipp HP (2002) Knockout mice: Simple solutions to the problems of genetic background  
598 and flanking genes. *Trends Neurosci* 25:336–340.

599 Wood GE, Shors TJ (1998) Stress facilitates classical conditioning in males, but impairs classical conditioning in  
600 females through activational effects of ovarian hormones. *Proc Natl Acad Sci U S A* 95:4066–4071.  
601

